Synthesis and characterization of Ga_2O_3 and In_2O_3 nanowires

Author: Alex Rodríguez Iglesias
Advisor: Guillem Domènech Gil and Albert Romano Rodríguez
Facultat de Física, Universitat de Barcelona, Diagonal 645, 08028 Barcelona, Spain.*

Abstract: Vapour-Liquid-Solid (VLS) mechanism is employed to grow Ga_2O_3 and In_2O_3 nanowires (NWs) using Ga_2O_3:C, In_2O_3:C and metallic In as precursor materials. A first attempt to fabricate heterostructures of Ga_2O_3/In_2O_3 NWs is also presented, by growing In_2O_3 NWs on previously grown Ga_2O_3 NWs. The NWs have been structurally characterized with Scanning Electron Microscopy and X-Ray diffraction. Moreover, gas sensors based on individual Ga_2O_3 NWs have been fabricated and tested under different concentrations of relative humidity diluted in synthetic air, demonstrating effectiveness in gas sensing.

I. INTRODUCTION

Crystalline Gallium oxide (Ga_2O_3) and Indium oxide (In_2O_3) are both n-type semiconductors with a band-gap of 4.9 eV and 3.6 eV at T = 300 K, respectively. Generally, semiconducting metal oxides have a superficial nanometric layer with oxygen vacancies, useful for gas sensing, as oxygen atoms from the gas can interact with the surface of the material. This interaction leads to a change in the conductivity of the semiconductor. Therefore, changes in the measured resistance can be related to the gas presence near the sensing material. A way to maximize the sensor's response is the optimisation of the surface-to-volume ratio. Several structures can be developed for this purpose, like nanorods, nanooctahedrons or NWs. Among them, the NW form is the most effective due to its higher surface-to-volume ratio and because of the difficulty of fabricating sensing devices with the other two.

NWs can be formed by different mechanisms. Among them, the VLS [1] mechanism has been selected because it has been widely used and has shown good results in the synthesis of Ga_2O_3 [2] and In_2O_3 [3] NWs.

In this work, Ga_2O_3 and In_2O_3 NWs are grown, using Ga_2O_3:C, In_2O_3:C and metallic In as precursor materials, with a Lindbergh furnace. The reason behind the synthesis of In_2O_3 NWs using In as precursor material is avoiding the use of graphite in the process. This could be useful to develop heterostructured Ga_2O_3 and In_2O_3 NWs by growing In_2O_3 on previously-fabricated Ga_2O_3 NWs without using graphite, which would eliminate the Ga_2O_3 NWs. A first approximation to a Ga_2O_3/In_2O_3 heterojunction is fabricated using the mentioned method. Furthermore, gas sensors based on individual Ga_2O_3 NWs have been fabricated and their response to synthetic air with different concentrations of relative humidity has been analysed.

II. EXPERIMENTAL PROCESS

A. NWs growth and characterization.

The VLS growth mechanism for the NWs formation is developed in a 5 cm diameter quartz tube inside a Lindbergh furnace, connected to four mass flow controllers (MFC) that control the gas flow injected from bottles filled with Ar, O_2 and a mixture of Ar and O_2 (with a concentration of 1000 ppm of O_2). The Lindbergh furnace has three programmable zones that allow heating each of them independently up to 1000 ºC, and with a maximum difference of about 150 ºC between adjacent zones.

The growth process consists in several steps. In the first part of the process, the precursor material is evaporated and transported along the quartz tube by a constant gas flow. When the precursor, in gas phase, reaches the samples, it is absorbed by the Au liquid drops formed on the substrates. When supersaturation takes place in the drops, the precursor precipitates at the Au-substrate interface forming the NWs. The three steps of this process are represented in Fig.1.

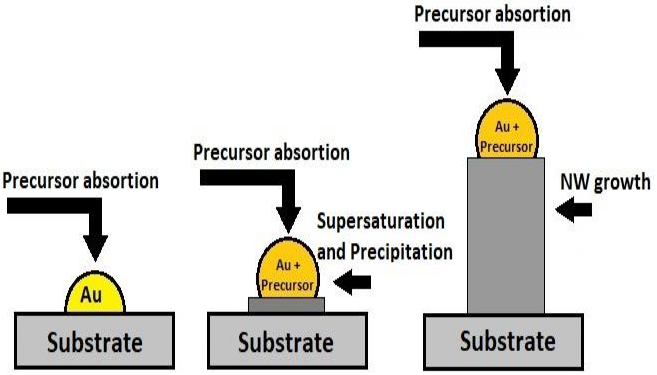

FIG.1. Scheme of the NWs growth according to the VLS mechanism.

Under specific conditions the Vapour-Solid (VS) [4] growth mechanism can also occur during the In_2O_3 NW growth process. The VS mechanism consists in the formation of solid structures in the gas phase, caused in our experiments by a high concentration of oxygen in the transport gas.

The growth was programmed in three phases, the first one (30 min long) corresponds to the increase of the temperature, in which the evaporation of the precursor and the formation of the Au drops begin. During the second step (of 1 hour) the temperature is maintained allowing the NWs growth. Finally, the furnace is left to cool down (during 2h) to room temperature. Prior to the process, a 0,06 ± 0,02 torr vacuum was made inside the tube to optimise oxygen concentration and minimise the water vapour content during the NW growth.

The substrates used are Si/SiO_2 5x5 mm^2 pieces, sputter-covered with a non-continuous Au layer of ~2 nm. During the heating step, Au agglomerates in droplets once above its melting temperature. Experiments with substrates without gold have also been carried out to study the viability of the growth avoiding the metallic droplets.

* Electronic address: arodriig15@alumnes.ub.edu

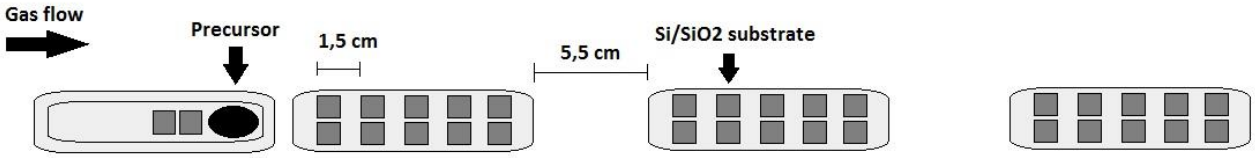

FIG.2. Sketch of the substrates distribution in the furnace.

The substrates are distributed in two rows of five pieces on three alumina plates. Two more substrates are located in the first alumina plate, where the precursor is placed, as schematically drawn in Fig.2.

The precursors used in the different processes were: 0.45g of Ga_2O_3 powder mixed with graphite in a 1:1.5 weight proportion, 0.25g of In_2O_3 powder mixed with graphite in a 4:1 weight proportion and 0.15 to 0.20g of a metallic In piece. The mixture with graphite is used to increase the vapour pressure of the precursors according to the carbothermal reduction process [5]. A flow of 100 standard cubic centimetres (sccm) of Ar or mixtures of Ar and O_2 at different concentrations is employed to transport the precursor material in gas phase along the tube. Ar is used as carrier gas to study the NW growth with In_2O_3 and Ga_2O_3 powder precursors and Ar/O_2 mixtures are used for the NW synthesis from In precursor. The optimal concentration of the transport gas for the growth of In_2O_3 NWs using In as precursor was found to be 100 ppm of O_2 diluted in Ar.

During the experiments the temperatures were set at 900/750/600 ºC for the In_2O_3 NW growth processes and at 950/800/650 ºC for the Ga_2O_3 case, respectively for the three zones of the CVD furnace.

The as-grown nanostructures were studied using a Jeol-7100 Field Emission Scanning Electron Microscope, operating at 15 keV, and equipped with an Energy Dispersive X-ray spectrometer (EDS). Two samples, one containing NWs of Ga_2O_3 and one of In_2O_3, obtained from Ga_2O_3:C and In_2O_3:C powders respectively, were analysed with a PANalytical X'Pert PRO MRD X-Ray diffractometer. The measurements were done under Grazing Incidence X-ray Diffraction (GIXRD) to maximize the interaction with the NWs from the surface.

B. Gas sensor characterization:

Due to the interaction between the superficial oxygen vacancies of the metal oxides with reducing and oxidizing gases from the surrounding atmosphere, variations in the conduction channel of the semiconducting NWs occur, which are detected as a change in the resistance of the device. For n-type semiconductors, reducing gases cause oxygen desorption from the surface, enlarging the conduction channel and reducing its resistance. Oxidizing gases induce the opposite process, an accumulation of negative charge in the surface, which reduces the section of the conducting channel increasing the resistance of the material.

In order to use the Ga_2O_3 NWs as gas sensors, the substrates were immersed in a vial with 200 µl of pure (96%) ethanol and then introduced in an ultrasonic bath to remove the NWs from the substrate. Next, the solution was deposited using a micro pipette on top of several micro hotplates (MHP), containing Pt electrodes on the surface and a buried heater that allows reaching temperatures up to 300 ºC in the centre of the MHP. The NWs dispersed on top of the MHP were electrically contacted to the Pt electrodes using Focused Electron Beam Induced Deposition techniques. Finally, the chips containing MHPs with individually contacted NWs are placed on top of TO8 supports and wire-bonded to them. To perform the gas measurements, the fabricated sensors were introduced in a steel chamber connected to four MFC, that allow the flow control of different gas mixtures. This is performed applying low current values (5 nA) to avoid damage to the NWs by Joule heating. The response of the sensors towards gas introduced in the chamber is accounted by the variations of the resistance of the NWs. The response is defined as the change in resistance with the gas related to the original resistance [6]:

$$S(\%) = \frac{R_0 - R_{gas}}{R_0} \times 100 \qquad (1)$$

Dry synthetic air with different concentrations of relative humidity has been introduced in the chamber at a constant flow of 200 ml/min. All the system has been controlled with a LabVIEW program.

III. RESULTS AND DISCUSSION

A. Scanning electron microscopy

Figures 3 and 4 show the results of Ga_2O_3 and In_2O_3 NWs growth processes assisted by carbothermal reduction, respectively.

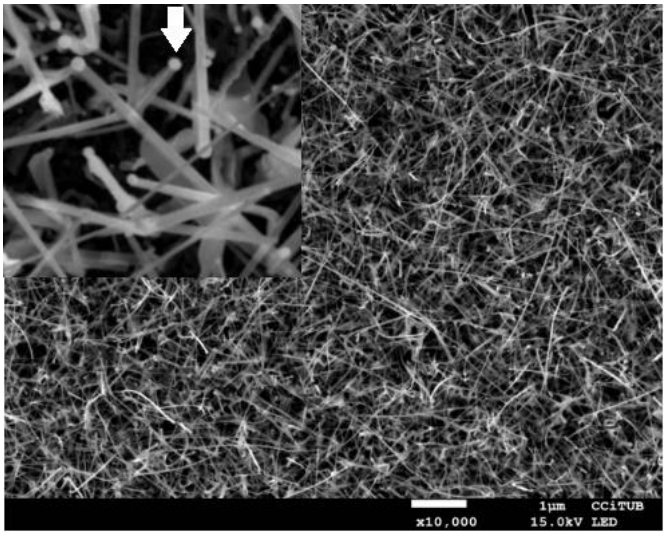

FIG.3. SEM image of the Ga_2O_3 NWs grown from Ga_2O_3:C powder. The inset is a higher magnification in which the gold tips can be identified (arrow).

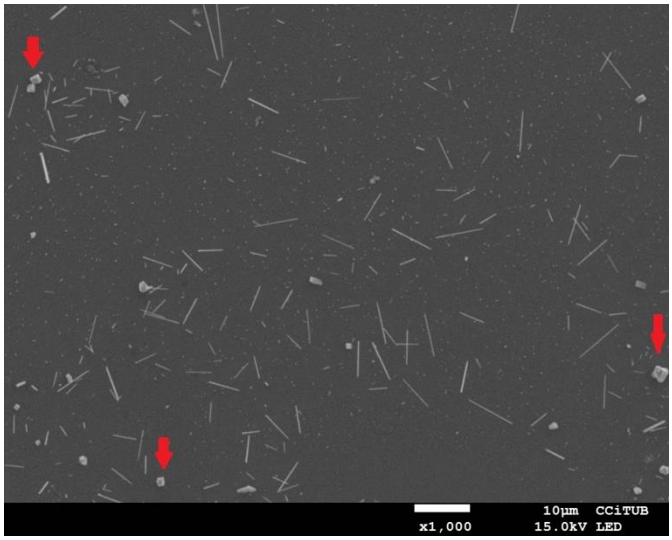

FIG.4. SEM image of In_2O_3 NWs grown from In_2O_3:C powder.

A large amount of NWs up to 20 µm long and diameters <100 nm can be observed in Fig.3. Gold drops can be seen in the inset (arrow), confirming that, with the conditions used, the VLS growth mechanism takes place using Ga_2O_3 powder mixed with graphite.

Similar results are observed in Fig.4, with NWs presenting lengths between 5 and 15 µm and diameters from 100 to 300 nm. It is noticeable that In_2O_3 NWs appear with a much lower density than Ga_2O_3. Other structures (pointed with arrows) produced by a VS process can also be observed.

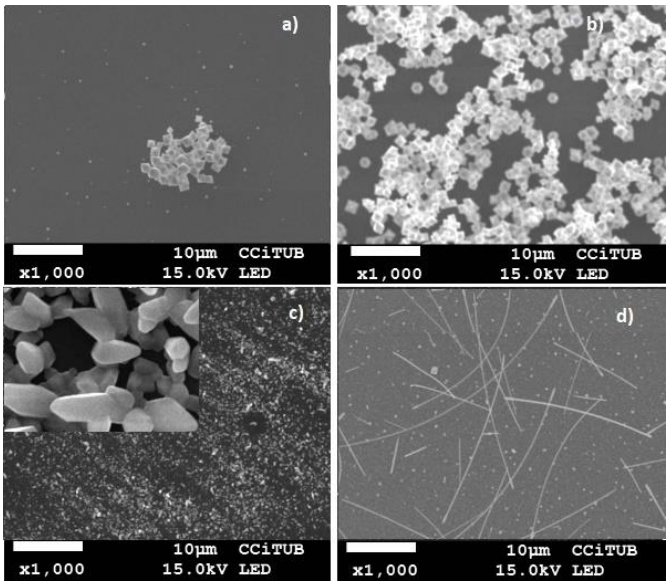

FIG.5. In_2O_3 NWs grown from metallic In under different conditions: a) 500 ppm of O_2, b) 800 ppm of O_2, c) and d) 100 ppm of O_2 and c) without the gold layer.

In figure 5, In_2O_3 NWs grown from metallic In precursor are shown, where different situations can be observed. When the O_2 concentration in the gas is above 500 ppm (Fig.5a and Fig. 5b) the Vapour-Solid (VS) mechanism dominates and mainly octahedral In_2O_3 structures are formed. Furthermore, it is also observable that an increase in the O_2 concentration leads to an increase in the density of octahedra. This is consequence of the VS mechanism, which forms the In_2O_3 octahedral structures in a reaction that needs O_2 to be produced and thus, a higher O_2 concentration promotes a higher amount of these structures.

When the O_2 concentration in the carrier gas is around 100 ppm, In_2O_3 NWs up to 20 µm long are formed on the substrates with the gold tips with similar density as the ones synthetized from the In_2O_3:C powder (even though Fig.5d seems to have larger density, it is an optical effect, consequence of the longer In_2O_3 NWs that appear in this case). These results prove that In_2O_3 NWs can be equally grown using either In_2O_3:C powder or metallic In as precursors and, therefore, metallic In can be useful for growing composite Ga_2O_3/In_2O_3 NWs, as mentioned above.

Using the same conditions (100 ppm of O_2), the substrates without the gold catalyst show only nanorod formations (fig 5c). A higher magnification can be observed in the inset of this figure. These observations prove that the Au drops promote the NWs growth via VLS mechanism.

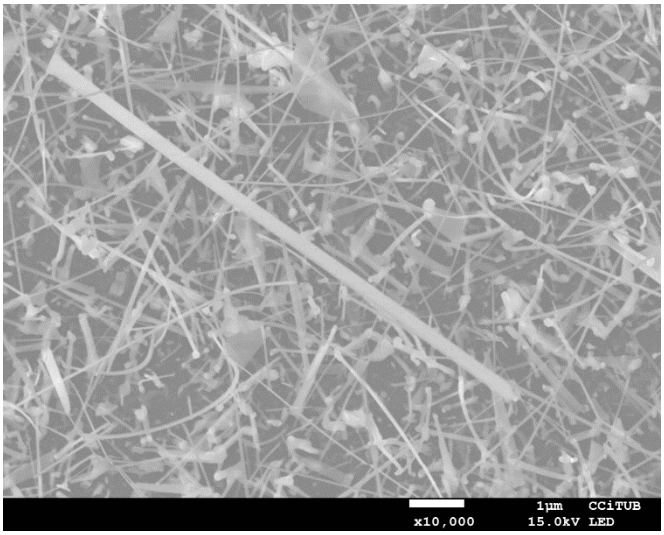

FIG.6. Composite Ga_2O_3/In_2O_3 NWs grown from Ga_2O_3:C powder and metallic In through a sequential growth, growing In_2O_3 NWs on top of the Ga_2O_3 NWs fabricated before.

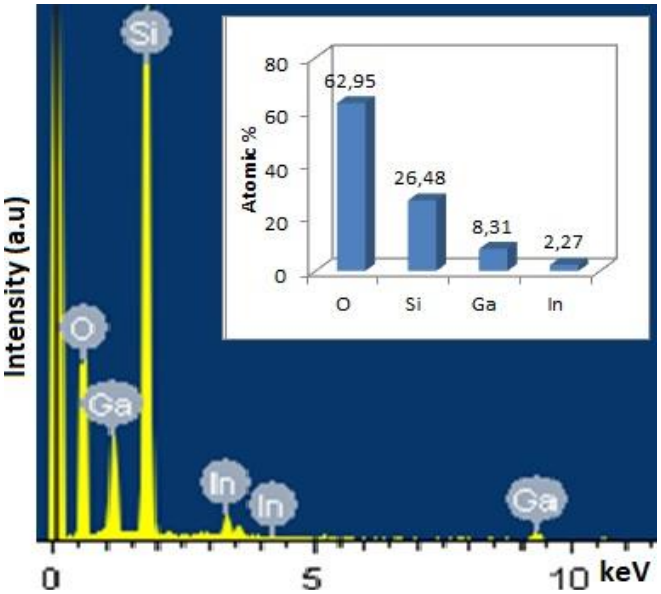

FIG.7. Energy-Dispersive X-Ray (EDS) spectrum from the zone of the sample shown in figure 6. The inset contains the atomic % of the four elements present in the sample.

Figures 6 and 7 show the results of the successive Ga_2O_3 and In_2O_3 NWs growth processes. Comparing the Ga_2O_3 sample obtained with Ga_2O_3:C powder (Fig.3) and Fig.6 several comments can be made. First, the diameter of a large number of the NWs in Fig.6 is larger than that of the Ga_2O_3 NWs of Fig.3. Second, solid formations larger than the NWs diameters are found at the tips of the NWs whereas in the Ga_2O_3 NWs only Au tips with diameters similar to those of the NWs are found. Last, large, straight and wide NWs also appear in the samples (as the diagonal one observed in Fig.6) in a very low density and in an inhomogeneous way.

Taking into account all these observations and the EDS spectrum, several statements can be proposed.

From these results it is clear that the Ga_2O_3 NWs did not shrink or disappear as a consequence of the In_2O_3 growth process, situation which was observed in previous studies carried out in this group, in which the sequential growth was performed using Ga_2O_3:C followed by In_2O_3:C. Therefore, doing the second step of the process with metallic In as precursor material has proven to be useful to grow indium-containing structures in samples that contain Ga_2O_3 NWs. Moreover, the EDS spectrum shows a Ga:In approximate proportion of 4:1 in the sample. The In content is expected to be in the form of In_2O_3, but further measurements need to be carried out to confirm it. No signal of C was detected, which is always present in the Ga_2O_3 samples coming from Ga_2O_3:C powder. Probably all carbon content dissapeared during the second process.

Additionally, the larger diameter observed in the NWs from Fig.6 could be a consequence of a core-shell structure formed by the In_2O_3 around the Ga_2O_3 NWs. The solid structures present at the tips of the NWs, not observed in the Ga_2O_3 NWs samples used as substrates for the second growth process, resemble In_2O_3 well-known structures. These structures could have grown at the tips of the Ga_2O_3 NWs being adsorbed by the gold droplet. Lastly, the widest and straightest NWs, occasionally observed after the sequential growth, are probably In_2O_3 NWs grown via VLS mechanism from gold drops at the substrate with no Ga_2O_3 content or from the tips of the Ga_2O_3 NWs, as shown in Fig.6 with a thick NW which seems to begin in a narrow Ga_2O_3 NW.

B. X-Ray diffraction (XRD)

Figures 8 and 9 show the XRD spectra of both Ga_2O_3 and In_2O_3 samples synthetized from Ga_2O_3:C and In_2O_3:C, respectively.

The measured Ga_2O_3 spectrum perfectly matches the reference spectrum of this material (JCPDS ref.: 41-1103) and, thus, confirms the monoclinic crystalline structure.

The In_2O_3 spectrum presents an almost perfect match with the reference file (JCPDS ref.: 6-416) and, thus, confirms that the grown In_2O_3 NWs have cubic crystalline structure. In this sample, some additional peaks not related to In_2O_3 can be identified, namely those at $2\theta = 23.5^\circ$ and $2\theta = 70.6^\circ$, marked in Fig. 9 with a red line. These peaks can be associated to an $AuIn_2$ alloy (JCPDS ref.: 3-65-2993) which has its main peaks at $2\theta = 23.6^\circ$, 39.07°, 46.17°, 56.45°, 62.04° and 70.79°. The two mentioned peaks (at 23.5° and 70.6°) fit with the reference for $AuIn_2$. The other four present some overlap to peaks of In_2O_3 and could be responsible for a larger width of the In_2O_3 peaks. The reason for the appearance of such an intense $AuIn_2$ XRD peaks could possibly be the presence of the Au drop at the tips of the NWs.

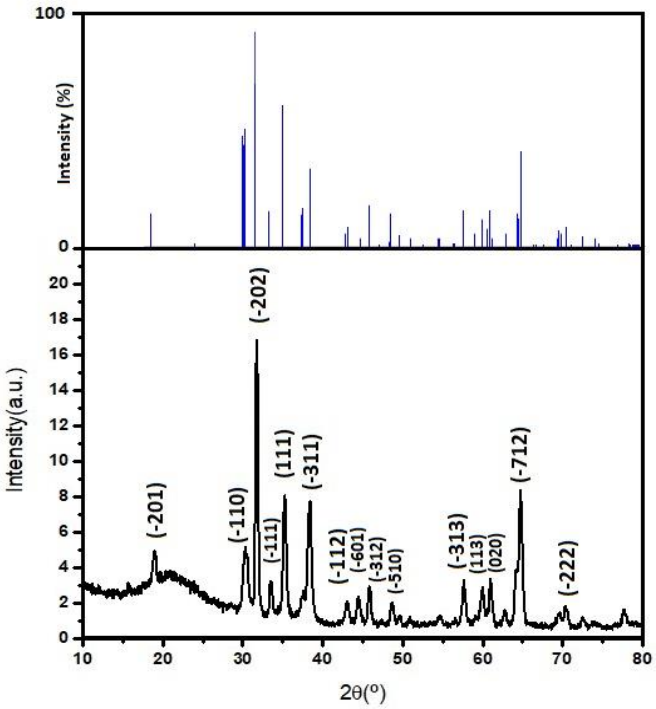

FIG.8. XRD Ga_2O_3 spectrum with the reference spectrum of the monoclinic Ga_2O_3 above.

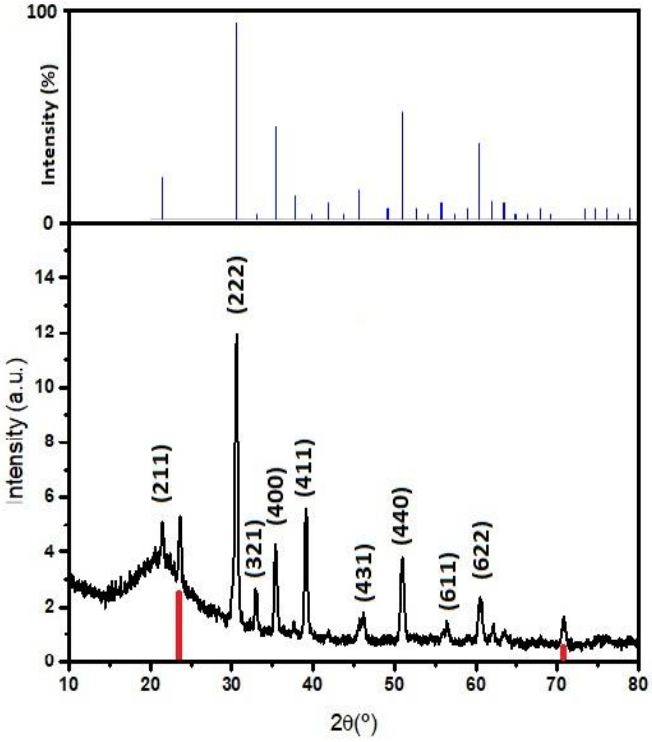

FIG.9. XRD In_2O_3 spectrum, together with its reference file corresponding to cubic In_2O_3.

Lastly, a difference between the heights of some peaks when compared to their respective reference spectra is clearly visible in both diagrams. This fact can be explained because

the NWs growth occurs along certain preferential crystallographic directions.

C. Sensing results

Figure 10 shows the resistance evolution of one of the fabricated gas sensors based on individual Ga_2O_3 NWs towards a pulse of 5 minutes with a relative humidity (RH) concentration of 50 % diluted in dry synthetic air.

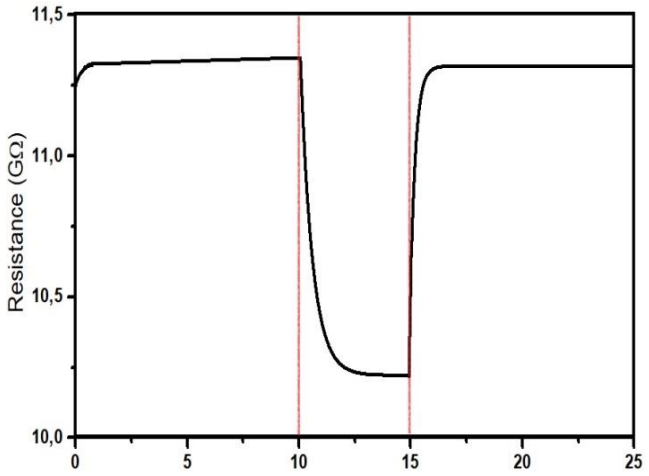

FIG.10. Resistance variation of the Ga_2O_3 NW to a 5-minute pulse of SA with a 50% RH. The pulse is indicated with the red lines.

The results show a decrease of the resistance of 1.13GΩ when the RH pulse is introduced in the gas test chamber, followed by the recovery of the baseline after the gas extraction. The gas interaction with the NW surface gives rise to a response of S = 10 %, according to equation (1). This result is in agreement with the expected behavior of Ga_2O_3, being an n-type semiconductor material. RH acts as a reducing gas that increases the section of the conducting channel of the NW and, therefore, reduces its resistance.

IV. CONCLUSIONS

In this work, the growth of Ga_2O_3 and In_2O_3 NWs via VLS mechanism, using Ga_2O_3:C, In_2O_3:C and metallic In as precursor materials, has been carried out. Different structures, like nanorods and octahedra, produced by a VS mechanism, have been formed when using metallic In due to the absence of Au drops and to the high concentration of O_2. This has allowed obtaining an optimal condition of 100 ppm of O_2 for growing the In_2O_3 NWs. Structural characterisation using SEM and XRD has been done and the results have confirmed the growth of monoclinic Ga_2O_3 NWs and cubic In_2O_3 NWs.

First attempt to fabricate heterostructures of Ga_2O_3/In_2O_3 NWs, growing In_2O_3 NWs on top of the previously formed Ga_2O_3 NWs, has been achieved employing the experimental conditions used in the growth process based on metallic In. The results seem to point towards the formation of a core-shell Ga_2O_3/In_2O_3 heterostructure, but further characterisation needs to be done to confirm the exact configuration.

Finally, gas sensors based on individual Ga_2O_3 NWs have been fabricated and tested against relative humidity diluted in synthetic air, proving its effectiveness as gas sensors.

Lastly, I would like to say that this work has helped me to improve my knowledge in physics obtained during the bachelor degree.

V. ACKNOWLEDGMENTS

First, I would like to acknowledge Guillem Domènech for teaching me the processes of fabrication and characterisation of Ga_2O_3 and In_2O_3 NWs developed in this work, and for the constant help he has provided me during these last three months. Secondly, I would like to acknowledge Albert Romano for his useful advices and supervision during the entire project.

Lastly, I would like to thank my family and friends for their support during these last months to finish my degree project.

[1] R.S. Wagner & W.C. Ellis, «Vapour-Liquid-Solid Mechanism of Single Crystal Growth,» *Applied Physics Letters*, vol. 4, no. 5, pp. 89–91, 1964.

[2] G. Domènech-Gil & I. Peiró & E. López Aymerich & M. Moreno & P. Pellegrino & I. Gràcia & C. Cané & S. Barth & A. Romano-Rodriguez, «Room Temperature Humidity Sensor Based on Single β-Ga_2O_3 Nanowires,» *Proceedings*, vol. 2, pp. 958-959, 2018.

[3] G. Domènech-Gil & J. Samà & P. Pellegrino & S. Barth & I. Gràcia & C. Cané & A. Romano-Rodriguez, «Gas Sensors Based on Individual Indium Oxide Nanowire,» *Sensors and Actuators B: Chemical*, vol. 238, pp. 447-454, 2016.

[4] N. Akhiruddin & R. Muhammad & Y. Wahab & Z. Ibrahim, «Growth of ZnO Nanowires by Vapour Solid Mechanism,» *Solid State Phenomena*, vol. 268, pp. 249-253, 2017.

[5] C.N.R Rao & G. Gundiah & F.L. Deepak & A. Govindaraj & A.K. Cheetham, «Carbon-assisted Synthesis of Inorganic Nanowires,» *Journal of Materials Chemistry*, vol. 14, pp. 440-450, 2004.

[6] J. Samà & S. Barth & G. Domènech-Gil & J.D. Prades & A. Romano-Rodríguez & N. López & O. Casals, et al., « Site-selectively Grown SnO_2 NWs Networks on Micromembranes for Efficient Ammonia Sensing in Humid Conditions,» *Sensors and Actuators B*, vol. 32, pp. 402-409, 2016.